Egyptian Journal of Chemistry
http://ejchem.journals.ekb.eg/

Waste-Derived Sodium Vanadate Nanostructures As Robust And Efficient Supercapacitor Electrodes

Hayat H. El Agamy [a] and Ahmed G. El-Deen [b]*

[a]Production Sector, Semi-Pilot Plant Department, Nuclear Materials Authority, 530 El-Maadi, Cairo, Egypt.
[b]Renewable Energy Science and Engineering Department, Faculty of Postgraduate Studies for Advanced Sciences (PSAS), Beni-Suef University, Beni-Suef 62511, Egypt.

In Loving Memory of Late Professor Doctor ""Mohamed Refaat Hussein Mahran""

Abstract

A sustainable, eco-friendly, and economical approach to recycling fly ash from power stations that burn heavy oil into sodium vanadate nanostructures. Various nano-shapes of the Na-vanadates were successfully prepared and then elucidated using different characterization techniques. The prepared Na-vanadate (NaV6O15) nanostructures were employed as electrode materials for supercapacitor applications. To evaluate the electrode performance, electrochemical measurements of three nanostructured sodium vanadate electrodes were conducted with cyclic voltammetry (CV) and galvanostatic charging-discharging (GCD) techniques in a 1 M Na2SO4 electrolyte. Among all formulation shapes of the synthesized Na-vanadates, the NaV6O15 with a rod-like structure (NVO-NRs) achieved a remarkable specific capacitance of 410 F/g at 1A/g. Additionally, it demonstrated an exceptional cycling life with 94% retention over 10000 continuous cycles. The (NVO-NRs) exhibited a superior energy density of 65.9 wh/kg at a power density of 500 w/kg. Overall, the prepared (NVO-NRs) electrode supplies durable, long-lasting, and efficient materials for supercapacitor applications.

Keywords: Sodium vanadate, Hydrothermal process, Nanostructured electrodes, Supercapacitors

1. Introduction

Excessive reliance on non-renewable and overexploitation of fossil fuels poses a significant danger to ecosystems worldwide. As a result, we must support the growth of renewable energy sources and work to reduce our reliance on fossil fuels [1]. Sustainable and renewable energy source innovation has lately garnered a lot of interest throughout the entire globe [2]. Batteries and supercapacitors can store energy because of how efficient they are. Rapid charging and discharging, excellent power density, enormous storage capacity, and a long lifespan are just a few of the many desirable characteristics of supercapacitors[3–5]. Two primary categories of supercapacitors exist based on the processes they use: electric double-layer capacitors (EDLCs) and pseudocapacitors. Supercapacitors with promising potential provide a range of desirable characteristics. These supercapacitors are used in several popular portable electronic gadgets. Examples include hybrid automobiles, laptops, toys, and mobile phones [6–8].

Several scientists have tried to create nanoscale electrode materials before as the size of the active material greatly affects its electrochemical efficiency[9,10] Supercapacitors have been constructed using a wide variety of materials, including carbonaceous form carbonaceous form[11], metal phosphides/sulfides/hydroxides[12–14] ,and transition metal oxides (TMOs)[15–17]. Transition metal oxides are top choices for pseudocapacitive electrode materials because they are eco-friendly, have a large specific surface area, are electrically conductive, have electroactive sites, and are chemically stable[18,19].

The TMO's ability to sustain various oxidation states and exhibit reversible redox reactions on its surface, close to the electrolyte, leads to an improvement in the efficiency and speed of charge storage transfer[20]. Several metal oxides have been employed , such as Fe_2O_3, RuO_2, SnO_2, MnO_2, and V_2O_5[21–26]. Due to its exceptional capacitive responsiveness, RuO_2 has garnered significant interest as a potential contender for supercapacitors. Nevertheless, its high cost and detrimental impact on

* Corresponding author: ag.eldeen@psas.bsu.edu.eg
Receive Date: 21 December 2023, Revise Date: 27 January 2024, Accept Date: 02 February 2024
DOI: 10.21608/ejchem.2024.256971.9013
©2024 National Information and Documentation Center (NIDOC)

the environment pose significant drawbacks [27]. Among the many transition metal oxide materials, compounds containing vanadium, such as V_2O_5 and V_6O_{13} are particularly noteworthy. This material has all the makings of a great supercapacitor: a high theoretical capacitance, low toxicity, a layered structure, inexpensive cost, and a variety of oxidation valences (V^{2+}, V^{3+}, V^{4+}, and V^{5+})[28].

Metals from the alkali earth series have two valence electrons and high electrical conductivity. Sodium, magnesium, zinc, and lithium-ion batteries are rechargeable and use a lot of vanadium oxide, an alkali earth metal AV_xO_y (A =Na, Mg, Ca)[29,30].

Nanomaterials based on the alkali earth metal vanadium have received little attention and research from a supercapacitor perspective. Amol Vedpathak et al. (2023) discovered that sodium vanadate (NVO) nanobelts exhibit normal capacitive behavior and a specific capacitance of 455 F/g at 0.5 A/g [31], which led them to adopt these nanobelts as electrode materials for supercapacitor (SC) applications. The unique design could lay a vital foundation for improving the electrochemical characteristics. Therefore, selecting materials with a shape-changing capability for high-performance charge storage is frequently advocated while investigating electrodes for supercapacitors.

In this research, utilizes the synthesized sodium vanadate (NVO) derived from fly ash as a promising storage material. The shape and size of sodium vanadate (NVO) nanorods, nanosheets, and nanoparticles have been properly controlled. These nanostructures possess desirable characteristics that make them very suitable for enhancing the performance of electrode materials in supercapacitors. The synthesis process incorporates green and facile hydrothermal, sol-combustion, and precipitation techniques. The fabricated NVO materials were employed to create efficient supercapacitors. The synthesized materials pose remarkable candidates for supercapacitors especially the NVO-NRs electrode achieved excellent specific capacitance and delivered great energy/ power densities.

2. Experimental

2.1. Materials

Waste-fly ash was collected from the “Assiut power plant in Egypt” and then performed by alkaline leaching using sodium carbonate in a previous study[32]. During fabrication, ultra-pure chemical reagents were used without any further processing. We bought hydrochloric acid, urea, starch, and ethyl alcohol from SRL company (India). Other chemicals such as carbon acetylene black, a polyvinylidene difluoride (PVDF) binder, and dimethylformamide (DMF) were provided from Sigma Aldrich. In addition, Alfa Aesar supplied the graphite foil. We utilized de-ionized (DI) water throughout the whole process.

2.2. Preparation of sodium vanadate nanostructures

2.2.1. Precipitation Synthesis

Mixing 100 ml of a starch solution containing 1% NaV_3O_8 into 100 ml of leach liquor with vigorously stirring for 75 minutes. Then, gradually add diluted hydrochloric acid (6 M) to the solution while stirring magnetically at 70 °C until the pH of the solution is adjusted to 2. Finally, filter and wash with distilled water and ethanol until free of chloride to complete the hydrolysis process. Afterward, the precipitates were oven-dried for a whole day at 100 °C. It was eventually necessary to anneal the dry sample at 500 ºC. You may see the precipitate process schematically shown in Figure 1.

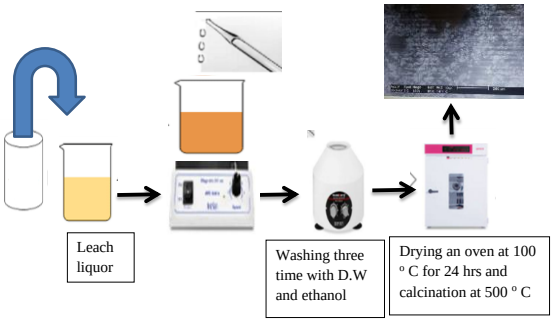

Figure 1. Schematic diagram of precipitate method

2.2.2. Hydrothermal synthesis.

Hydrolysis of a NaV_3O_8 solution was accomplished by bringing the leaching liquid's pH down to 2 with the slow addition of diluted hydrochloric acid (6 M). The resulting mixture was then cooked in a 50 mL autoclave to 180 ºC for a duration of 12 hours. Afterwards, it was dried in an oven set at 100 °C for 24 hours after being rinsed many times with ethanol and deionized water. Once the sample had dried, the last step was to heat it to 500 ºC. This hydrothermal analysis is illustrated in Figure 2.

2.2.3. Self-combustion synthesis

The leach liquor may be made into a clear yellow solution by adding NaV_3O_8 and hydrochloric acid (6 M) and stirring until the pH drops to 2. Right after 10 g of urea fuels were added, the solution became blue, leaving behind a dark green hue. Eventually, the gel was heated to the point where it underwent a quick and self-sustaining combustion process, which produced the powder. Before drying for 24 hours in an oven at 100 ^{C}, the product was cleaned many times with deionized water. Annealing was then performed

on it for four hours at 500 ºC. It was eventually achieved to get the NVO powder that had a dark brown color. The mechanism of self-combustion is shown schematically in Figure 3.

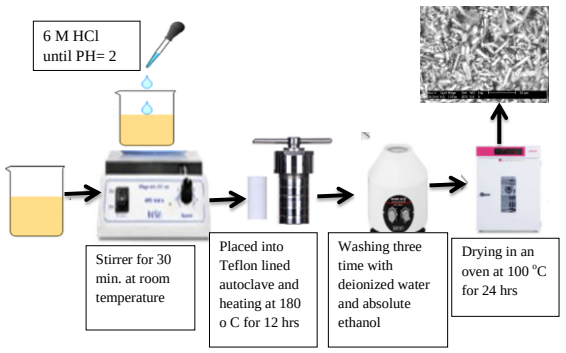

Figure 2. Schematic diagram of hydrothermal method

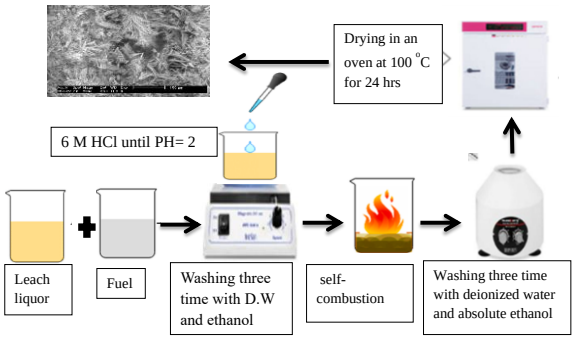

Figure 3. Schematic diagram of self-combustion method

2.3. Characterizations

An X-ray diffractometer (Mini Flex 600 -Rigaku, Japan) was employed to examine the crystal structure and purity of the obtained powder. Scanning electron microscopy (LEO 1450 VP) and transmission electron microscopy (JEOL JEM-2100) both run at an accelerating voltage of 2000 V were employed to analyze the nanostructures' shapes.

2.4. Electrode fabrication and electrochemical testing

The electrodes have been created using a mass ratio of 85:8:7 of active materials, powdered carbon black, and PVDF mixed well in dimethylformamide (DMF). Soon after, everything was blended into a homogenous slurry using a high-speed mixer. The electrode components were distributed onto a clean, compacted sheet of graphite foil using a thin film roller. Then, they were dried at 100 °C for a whole night to eliminate any solvent, resulting in a final mass of 1.2 mg/cm^2.

An experimental setup consisting of a half-cell, three-electrode system, 1 M Na_2SO_4, coated active materials on graphite foil, an Ag/AgCl electrode, and a counter Pt plat electrode served for evaluating the electrochemical performance of the created electrode materials. An OrigaFlex-(OGF-500, France) electrochemical workstation was used to conduct charging/discharging tests and cyclic voltammetry (CV) on the produced electrodes at voltages ranging from 0 to 1 V. For the active material in the electrode, the specific capacitance (C, F/g). and energy/power density (E, Wh/kg & P, W/kg), as seen by the charge-discharge curves, can be determined using the following formulae.

$$C = \frac{I \times \Delta t}{m \times \Delta V} \quad (1)$$

$$E = \frac{0.5\, C \Delta V^2}{3.6} \quad (2)$$

$$P = \frac{E * 3600}{\Delta t} \quad (3)$$

I reflect the specific current, Δt for the discharge time, m refers to the mass loading of the synthesized powder, and ΔV represents applied potential.

3. Results and discussion

3.1. Structural and Morphological shape

In Figure 4, X-ray diffraction patterns of sodium vanadate (NaV_6O_{15}) produced via precipitation hydrothermal and self-combustion methods are displayed. The XRD patterns show the formation of the monoclinic phase with characteristics peaks at 2θ of 9.8°, 12.4°, 29.3° and 41.2° corresponding to (NaV_6O_{15}) nanostructure with card no [PDF 24-1155)][33]. No noises nor other oxide peaks reflecting the impurity-free NVO powder were successfully synthesized. Figure 4 shows the crystal structure of NVO, which is a layered monoclinic phase. The multilayer NVO structure is made more stable by Na^+, which functions as a support between the layers. Also, ions may still be inserted into the sufficient gaps between the NVO layers[34]. The XRD pattern for the (NVO-NRs) sample demonstrated high-intensity and sharp peaks compared to (NVO -NPs) and (NVO-NSs) samples, reflecting the pure and high crystalline nature of the fabricated materials.

The morphology of the sodium vanadate nanostructures was observed by using SEM and TEM as shown in Figures 5 and 6. For surface morphological shape Figure 5a–c displays sodium vanadate nanostructure micrographs created by self-combustion, hydrothermal, and precipitation techniques. In Figure 5a, the precipitation method's micrograph demonstrates how nanoparticles are created. However, the micrograph of the hydrothermal approach in Figure 5b reveals a rod-

like structure. Because it allows for charge storage with a short ionic length and transportation directionality, this structure is ideal for usage in supercapacitors [3] and the micrograph of the self-combustion method in Figure 5c demonstrates a sheet-like morphology.

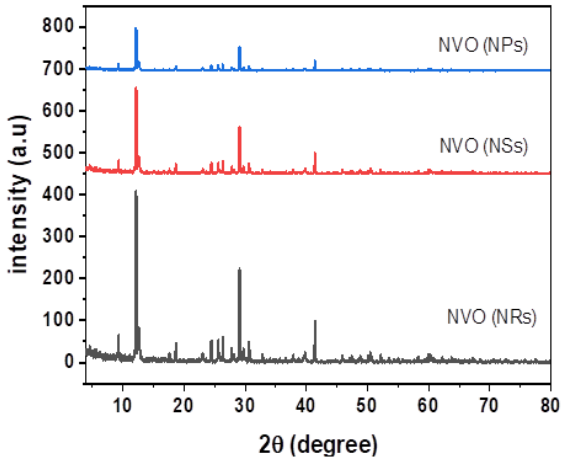

Figure 4. Powder XRD patterns of NaV_6O_{15} nanostructure made using various techniques (NVO(NSs) nanosheet by using Self-combustion, (NVO(NPs) nanoparticle by using precipitation and (NVO(NRs)) nanorods by using hydrothermal.

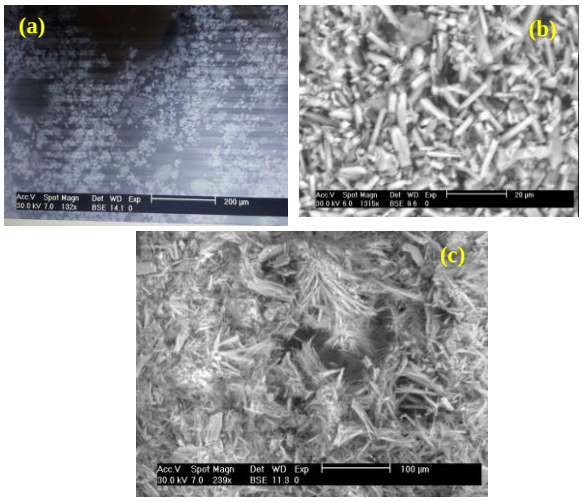

Figures 5 (a-c) SEM images for the different morphological shapes of sodium vanadate nanostructures

In Figures 6a-c, Figure 6a TEM image of NaV_6O_{15} nanoparticles produced by the precipitation approach is displayed. In Fig. 6 (b, a) TEM image of NaV_6O_{15} nanorods produced by the hydrothermal approach is displayed. From the TEM image of the combustion synthesized NaV_6O_{15} is composed of many sheets shown in Fig. 6c.

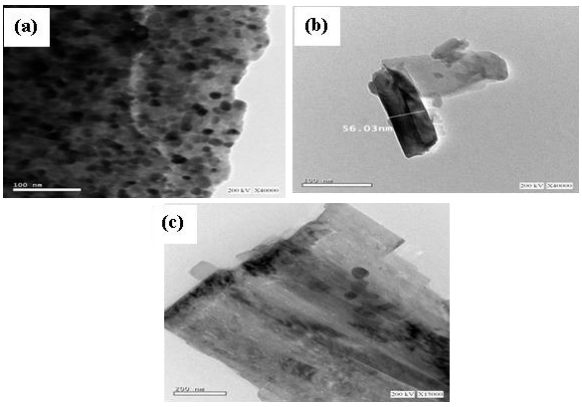

Figure 6 a-c TEM images of the prepared sodium vanadate nanostructures.

3.2. Electrochemical performance

To test the efficiency and capacitance of the sodium vanadate electrodes that were just manufactured, GCD and CV were performed in a three-electrode configuration in a 1 M Na_2SO_4 aqueous electrolyte. The CV curves of three different types of NVO nanoelectrodes; NPs, NRs, and NSs are shown in Fig.7(a) compared at 5 mV/s against Ag/AgCl in a voltage range of 0 to 1V. The pseudocapacitive behaviors seen by all of the CV curves, with their almost rectangular-shaped loops, indicate that the reactions are reversible and sequential. The (NVO-NRs) electrode, out of all the NVO electrode shapes tested, has the greatest current and the smallest redox hump, both of which point to the charge storage mechanism's capacitive faradic contribution[35]. Figure 7 (b) shows a comparison of the NVO-NRs electrode's CV curves at different sweep speeds. When scanning rapidly, the CV curves acquire a tiny oval shape, indicating rapid and reversible charge storage [33]. Under a particular current of 1 A/g, the GCD curves of all the sodium vanadate-based electrode materials that were synthesized are shown in Fig. 7(c). The GCD curves show that the manufactured (NVO-NRs) electrode usually has a much longer discharge duration than any of the other materials that were tested. The long axial ratio of the (NVO-NRs) electrode hinders the aggregation of particles for NVO-NPs and the formation of layers for NVO-NSs. This results in a significant enhancement in electrochemical capacitance, as seen by the CV and GCD measurements. Figure 7 (d) displays the GCD profiles of the (NVO-NRs) at various current densities, allowing for comparison. The fact that the form remains triangular and there is no infrared loss even at high current densities suggests excellent reversibility and excellent conductivity. Figure 7 (e) displays the specific capacitance of the manufactured electrodes at different particular currents. The NVO-NRs demonstrated an exceptional specific capacitance of 410 F/g, which is higher than the 278

F/g and 210 F/g achieved by the NVO-NSs and NVO-NPs, respectively, at 1A/g. The as-prepared NVO-NRs exhibit optimal pore size distributions, a high specific surface area, and low agglomeration characteristics, all of which contribute to the NVO electrodes' ability to adsorb ions throughout their rod-based structure, leading to their superior capacitance performance.

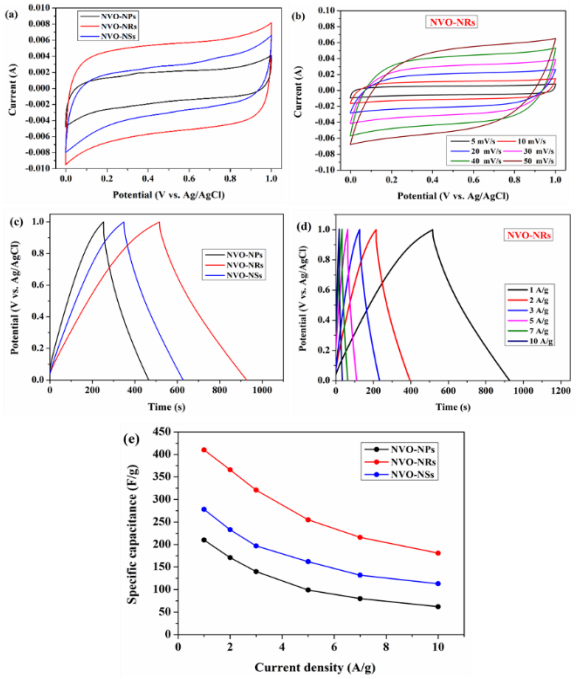

Figure 7 Electrochemical studies; (a) CV comparison for the fabricated electrode materials at a scan rate of 5 mV/s, (b) CV curves of the NVO nanorods at different scan rates. (c) GCD curves of the fabricated NVO nanostructures at a current density of (1A/g), (d) GCD profiles of NVO nanorods at various current densities, and (e) Specific capacitance performance versus current densities plot for the prepared electrode materials.

The stability of the system was tested by conducting 10,000 cycles of a charge/discharge process at 5 A/g. Fig. 8 (a) displays that the capacitance does not significantly decrease with cycling. The NVO-NRs electrode has remarkable electrochemical reversibility and chemical stability with an end-of-test cycle stability of 94%. The Ragone Plot, shown in Figure 8 (b), illustrates the connection between power densities and energy densities. The NVO-NRs electrode achieves its maximum energy density of 56.9 Wh/kg at a power density of 500 W/kg, and it continues to provide a comparatively high density of 25.1 Wh/kg even when the power density is increased to 5000 W/kg. As a result, the NVO-based rods that were manufactured had outstanding electrochemical performance, proving that they are a top contender for a promising electrode in energy storage applications.

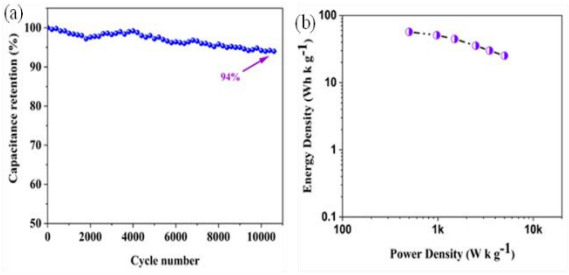

Figure 8 (a) cycling stability test and Ragone plot for the fabricated NVO-NRs supercapacitor electrode (b).

4. Conclusions

The manufacture of sodium vanadate nanostructures from waste fly ash was achieved utilizing simple and commonly utilized self-combustion. Electrodes with a range of (NaV_6O_{15}) nanostructures, including nanoparticles, nanosheets, and nanorods, were created. Cyclic voltammetry (CV), galvanostatic charge-discharge (GCD), and specific capacitances were used to evaluate the electrochemical efficiency for the produced materials electrode. At 1 A/g, the manufactured NVO nanorods had a maximum specific capacitance of 410 F/g, and they exhibited remarkable cycling stability, retaining 94% of their capacitance after 10,000 charge/discharge cycles. In addition, at 500 w/kg, the electrode made of NVO nanorods produced an outstanding energy density of 56.9 wh/kg. Converting fly ash waste into economical Electrodes constructed from NaV_6O_{15}nanostructures improved electrode features, making the material a suitable candidate for electrodes in sustainable hybrid supercapacitors that store energy on a massive scale for the grid.

5. Conflicts of interest

The authors declare that they have no known competing financial interests or personal relationships that could have appeared to influence the work reported in this paper.

6. References

[1] N.L. Panwar, S.C. Kaushik, S. Kothari, Renew. Sustain. Energy Rev. 15 (2011) 1513–1524.

[2] I. Dincer, Renew. Sustain. Energy Rev. 4 (2000) 157–175.

[3] W. Guo, C. Yu, S. Li, J. Qiu, Energy Environ. Sci. 14 (2021) 576–601.

[4] D. Majumdar, M. Mandal, S.K. Bhattacharya, Emergent Mater. 3 (2020) 347–367.

[5] B.K. Kim, S. Sy, A. Yu, J. Zhang, Handb. Clean Energy Syst. (2015) 1–25.

[6] S.S. Shah, M.A. Aziz, Z.H. Yamani, Chem. Rec. 22 (2022) e202200018.

[7] P.A. Shinde, Q. Abbas, N.R. Chodankar, K. Ariga, M.A. Abdelkareem, A.G. Olabi, J. Energy Chem. 79 (2023) 611–638.

[8] R. Kötz, M. Carlen, Electrochim. Acta 45 (2000) 2483–2498.

[9] A.G. El-Deen, M. El-Newehy, C.S. Kim, N.A.M. Barakat, Nanoscale Res. Lett. 10 (2015) 1–7.

[10] A.G. El-Deen, M. Hussein El-Shafei, M. Hussein El-Shafei, A. Hessein, A. Hessein, A.H. Hassanin, N.M. Shaalan, N.M. Shaalan, A.A. El-Moneim, A.A. El-Moneim, A.A. El-Moneim, Nanotechnology 31 (2020) 365404.

[11] S.A. Salheen, H.F. Nassar, S. Dsoke, A.G. El-Deen, Colloids Surfaces A Physicochem. Eng. Asp. 660 (2023) 130821.

[12] S. He, Z. Li, H. Mi, C. Ji, F. Guo, X. Zhang, Z. Li, Q. Du, J. Qiu, J. Power Sources 467 (2020) 228324.

[13] J. Gong, J. Yang, J. Wang, L. Lv, W. Wang, L. Pu, H. Zhang, Y. Dai, Electrochim. Acta 374 (2021) 137794.

[14] A.G. El-Deen, M.K. Abdel-Sattar, N.K. Allam, Appl. Surf. Sci. 587 (2022) 152548.

[15] M.A. Nassar, S.I. El-dek, W.M.A.E. Rouby, A.G. El-Deen, J. Energy Storage 44 (2021) 103305.

[16] P. Yu, W. Duan, Y. Jiang, Front. Chem. 8 (2020) 1–9.

[17] T. Xing, Y. Ouyang, Y. Chen, L. Zheng, C. Wu, X. Wang, J. Energy Storage 28 (2020) 101248.

[18] R. Kumar, S.M. Youssry, H.M. Soe, M.M. Abdel-Galeil, G. Kawamura, A. Matsuda, J. Energy Storage 30 (2020) 101539.

[19] B. Ding, X. Wu, J. Alloys Compd. 842 (2020) 155838.

[20] R. Kumar, S.M. Youssry, H.M. Soe, M.M. Abdel-Galeil, G. Kawamura, A. Matsuda, J. Energy Storage 30 (2020) 101539.

[21] R. Arunachalam, R.K.V. Prataap, R. Pavul Raj, S. Mohan, J. Vijayakumar, L. Péter, M. Al Ahmad, Surf. Eng. 35 (2019) 103–109.

[22] Y. Jin, M. Jia, Colloids Surfaces A Physicochem. Eng. Asp. 464 (2015) 17–25.

[23] P. Ning, X. Duan, X. Ju, X. Lin, X. Tong, X. Pan, T. Wang, Q. Li, Electrochim. Acta 210 (2016) 754–761.

[24] K. Orisekeh, B. Singh, Y. Olanrewaju, M. Kigozi, G. Ihekweme, S. Umar, V. Anye, A. Bello, S. Parida, W.O. Soboyejo, J. Energy Storage 33 (2021), 102042.

[25] H.A. Ghaly, A.G. El-Deen, E.R. Souaya, N.K. Allam, Electrochim. Acta 310 (2019) 58–69.

[26] S.M. Lee, Y.J. Park, D. Van Lam, J.H. Kim, K. Lee, Appl. Surf. Sci. 512 (2020) 145626.

[27] S. Chen, J. Zhu, X. Wu, Q. Han, X. Wang, ACS Nano 4 (2010) 2822–2830.

[28] D. Chen, J. Li, Q. Wu, J. Nanoparticle Res. 21 (2019) 1–15.

[29] V. Manev, A. Momchilov, A. Nassalevska, G. Pistoia, M. Pasquali, J. Power Sources 54 (1995) 501–507.

[30] S. Maingot, N. Baffier, J.P. Pereira-Ramos, P. Willmann, Solid State Ionics 67 (1993) 29–34.

[31] A. Vedpathak, T. Shinde, M.A. Desai, B.R. Thombare, R. Humane, S.A. Raut, R. Kalubarme, S.D. Sartale, S. Bhagwat, ACS Appl. Energy Mater. 6 (2023) 4693–4703.

[32] H.H. El-Agamy, Inorg. Nano-Metal Chem. (2023) 1–8.

[33] R. Li, C. Guan, X. Bian, X. Yu, F. Hu, RSC Adv. 10 (2020) 6807–6813.

[34] J.P. Pereira-Ramos, R. Messina, L. Znaidi, N. Baffier, Solid State Ionics 28 (1988) 886–894.

[35] W. Bi, X. Jiang, C. Li, Y. Liu, G. Gao, G. Wu, M. Atif, M. Alsalhi, G. Cao, ACS Appl. Mater. Interfaces 14 (2022) 19714–19724.